MCB
Journals.ASM.org

Aurora B Overexpression Causes Aneuploidy and p21^{Cip1} Repression during Tumor Development

Alejandra González-Loyola,[a] Gonzalo Fernández-Miranda,[a] Marianna Trakala,[a] David Partida,[a] Kumiko Samejima,[b] Hiromi Ogawa,[b] Marta Cañamero,[c] Alba de Martino,[c] Ángel Martínez-Ramírez,[d] Guillermo de Cárcer,[a] Ignacio Pérez de Castro,[a] William C. Earnshaw,[b] Marcos Malumbres[a]

Cell Division and Cancer Group, Spanish National Cancer Research Center, Madrid, Spain[a]; Wellcome Trust Centre for Cell Biology, University of Edinburgh, Edinburgh, United Kingdom[b]; Histopathology Unit, Spanish National Cancer Research Center, Madrid, Spain[c]; Cytogenetics Unit, M. D. Anderson Hospital, Madrid, Spain[d]

Aurora kinase B, one of the three members of the mammalian Aurora kinase family, is the catalytic component of the chromosomal passenger complex, an essential regulator of chromosome segregation in mitosis. Aurora B is overexpressed in human tumors although whether this kinase may function as an oncogene *in vivo* is not established. Here, we report a new mouse model in which expression of the endogenous *Aurkb* locus can be induced *in vitro* and *in vivo*. Overexpression of Aurora B in cultured cells induces defective chromosome segregation and aneuploidy. Long-term overexpression of Aurora B *in vivo* results in aneuploidy and the development of multiple spontaneous tumors in adult mice, including a high incidence of lymphomas. Overexpression of Aurora B also results in a reduced DNA damage response and decreased levels of the p53 target p21^{Cip1} *in vitro* and *in vivo*, in line with an inverse correlation between Aurora B and p21^{Cip1} expression in human leukemias. Thus, overexpression of Aurora B may contribute to tumor formation not only by inducing chromosomal instability but also by suppressing the function of the cell cycle inhibitor p21^{Cip1}.

Most human cancers contain aneuploid cells, and a significant number of studies have pointed to abnormalities in the regulation of mitosis as a contributing cause of chromosomal instability in tumors (1–4). Various defects in mitotic checkpoints, the anchoring of chromosomes to the mitotic spindle, chromosome cohesion, or the number of centrosomes can result in aberrant cell division leading to aneuploid daughter cells. Aurora kinase B (AurkB), one of the three members of the Aurora kinase family (5), is involved in many of these mitotic processes. Aurora B was first identified in *Saccharomyces cerevisiae* (as Ipl1) in a screen for mutants that display an increase in ploidy (6). This kinase is the catalytic subunit of the chromosomal passenger complex (CPC), which regulates key steps during mitosis, including chromosome interactions with microtubules, chromatid cohesion, spindle stability, and cytokinesis (7). Aurora B kinase plays a central role in correcting kinetochore attachment errors, including merotelic attachments, through the phosphorylation of kinetochore substrates, thus leading to the destabilization of incorrect attachments and allowing reorientation of the kinetochore toward the correct spindle pole (8, 9). It has been proposed that correct attachment requires fine-tuning of tension across sister kinetochores and that either increasing or decreasing Aurora B activity may cause merotelic and syntelic attachments, which in turn can lead to aneuploidy (5, 7, 10–12).

Aurora A, but not Aurora B, has been claimed to function as an oncogene *in vivo* by inducing mitotic abnormalities (13). Aurora B overexpression is common in human tumors, where elevated levels of the Aurora B transcript or protein are often associated with poor prognosis (14–22). Moreover, Aurora B is part of the CIN70 gene expression signature associated with high chromosome instability (CIN) in human cancers (23). Recent studies have also linked Aurora B activity with inhibition of the tumor suppressor p53 and decreased levels of its target genes although the relevance of this interaction *in vivo* has not been tested (24–26).

To understand the possible oncogenic function of Aurora B, we have generated a murine allele in which the expression of the endogenous Aurora B gene, *Aurkb*, can be hyper-induced *in vitro* and *in vivo*. This allele is based on the "promoter-hijack" strategy previously used in chicken DT40 cells in which the endogenous *Aurkb* promoter is replaced with a minimal promoter responsive to the tetracycline-inducible transactivator (rtTA) (27). Overexpression of Aurora B results in chromosomal instability and aneuploidy *in vitro* and *in vivo*. In addition, Aurora B overexpression is accompanied by a defective DNA damage response and impaired induction of the p53 target p21^{Cip1}. Long-term overexpression of Aurora B results in the development of multiple tumors, including spleen lymphomas or lung adenocarcinomas among others, suggesting that Aurora B overexpression may favor both aneuploidy and p21^{Cip1} downregulation during tumor development.

MATERIALS AND METHODS

Generation and characterization of Aurora B mutant mice. The inducible *Aurkb* allele was generated by using the promoter-hijack strategy (27). The conditional targeting construct contained a minimal *tetO*-cytomegalovirus (CMV) promoter (Tet-P) inserted in front of the *Aurkb* ATG, thus replacing the Aurora B endogenous promoter, and a puromycin

Received 22 October 2014 Returned for modification 11 November 2014
Accepted 29 July 2015
Accepted manuscript posted online 3 August 2015
Citation González-Loyola A, Fernández-Miranda G, Trakala M, Partida D, Samejima K, Ogawa H, Cañamero M, de Martino A, Martínez-Ramírez A, de Cárcer G, Pérez de Castro I, Earnshaw WC, Malumbres M. 2015. Aurora B overexpression causes aneuploidy and p21^{Cip1} repression during tumor development. Mol Cell Biol 35:3566–3578. doi:10.1128/MCB.01286-14.
Address correspondence to Marcos Malumbres, malumbres@cnio.es.

doi:10.1128/MCB.01286-14

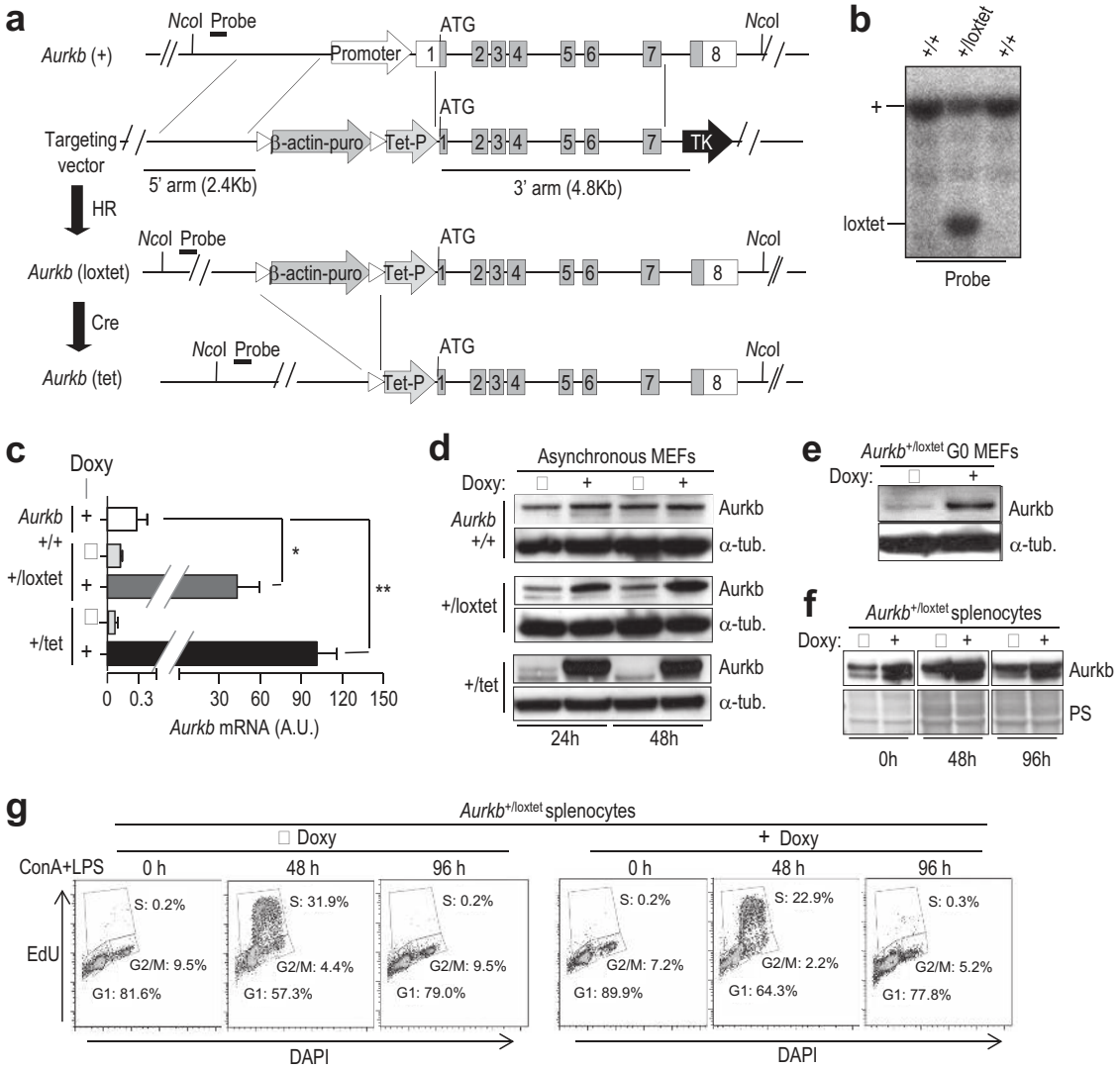

FIG 1 Generation and characterization of an endogenous Aurora B-inducible model. (a) Schematic representation of the alleles used in this study for the inducible overexpression of Aurora B (see Materials and Methods for details). In the *Aurkb*$^{lox\text{-}tet}$ allele, the Aurora B endogenous promoter was replaced by Tet-P, a minimal CMV promoter that contains seven in tandem repeats of *tetO* sequences recognized by the transactivator regulatory proteins rtTA. The activity of Cre recombinase resulted in the removal of the puromycin (puro) resistance cassette and the generation of the *Aurkb*^{tet} allele. HR, homologous recombination; TK, thymidine kinase. (b) Southern blot analysis of ES cell clones after homologous recombination, indicating the presence of the recombinant *Aurkb*$^{lox\text{-}tet}$ allele in one of the clones. The location of the probe is indicated in panel a. (c) Quantitative RT-PCR data from *Aurkb*$^{+/+}$, *Aurkb*$^{+/lox\text{-}tet}$, and *Aurkb*$^{+/tet}$ MEFs, carrying the *Rosa26*$^{M2rtTA/M2rtTA}$ allele, in the absence or presence of doxycycline (Doxy) for 48 h. GAPDH was used as a control of expression. Data are means ± standard deviations ($n = 3$ separate clones). *, $P < 0.05$; **, $P < 0.01$ (Student's *t* test). AU, arbitrary units. (d) Immunodetection of Aurora B in *Aurkb*$^{+/+}$; *Rosa26*$^{M2rtTA/M2rtTA}$, *Aurkb*$^{+/lox\text{-}tet}$; *Rosa26*$^{M2rtTA/M2rtTA}$ and *Aurkb*$^{+/tet}$; *Rosa26*$^{M2rtTA/M2rtTA}$ primary mouse embryonic fibroblasts (MEFs) stimulated with doxycycline. α-Tubulin (α-tub) was used as a loading control. (e) Aurora B levels in serum-starved *Aurkb*$^{+/lox\text{-}tet}$; *Rosa26*$^{M2rtTA/M2rtTA}$ MEFs treated or not treated with doxycycline for 48 h. α-Tubulin was used as a loading control. (f) Aurora B expression is significantly induced in *Aurkb*$^{+/lox\text{-}tet}$ resting (0 h) or concanavalin A plus lipopolysaccharide (ConA+LPS)-induced (48 and 96 h) splenocytes. PS, Ponceau S. (g) EdU incorporation and DNA content profiles in *Aurkb*$^{+/lox\text{-}tet}$ splenocytes before or after treatment with concanavalin A plus lipopolysaccharide (ConA+LPS). Data are representative of two separate experiments.

cassette for positive selection of the clones (Fig. 1a). After homologous recombination in embryonic stem (ES) cells, clones were selected using puromycin resistance, and *Aurkb*$^{+/lox\text{-}tet}$ clones were identified using Southern blot analysis (Fig. 1b). These ES cells were aggregated to generate *Aurkb*$^{+/lox\text{-}tet}$ mice, and the puromycin resistance cassette was removed *in vivo* by crossing these mice with transgenic mice expressing the Cre recombinase, resulting in the *Aurkb*^{tet} allele. The Rosa26 rtTA (*Rosa26*^{M2rtTA}) allele expresses a tetracycline-inducible M2rtTA transactivator driven from the endogenous ubiquitous Rosa26 promoter (28). Complete protocols, primers, and probes for genotyping are available from the authors upon request. For induction, mutant and wild-type mice were fed with doxycycline-supplemented food (Harlan Laboratories Models) after weaning. All animals were maintained in a mixed 129/Sv (25%), CD1 (25%), and C57BL/6J (50%) background. Mice were housed at a pathogen-free animal facility of the Centro Nacional de Investigaciones Oncológicas (CNIO; Madrid, Spain), according to the animal care standards of the institution. These animals were observed daily, and sick mice were euthanized humanely in accordance with the Guidelines for

Humane Endpoints for Animals Used in Biomedical Research. The Instituto de Salud Carlos III and the IACUC approved all animal protocols for animal care and research.

For histological analysis, dissected organs were fixed in 10% buffered formalin (Sigma) and embedded in paraffin wax. Sections of 3- or 5-μm thickness were stained with hematoxylin and eosin (H&E). Additional immunohistochemical examination of the tissues and pathologies was performed using specific antibodies against the following antigens: Aurora B (ab2254; Abcam), Ki67 (0003110QD; Master Diagnostica), active caspase 3 (AF835; R&D Systems), CD3e (M-20, sc-1127; Santa Cruz Biotechnology), phospho-p53 (Ser15; Cell Signaling), $p21^{Cip1}$ (sc-397-G; Santa Cruz Biotechnology), Pax-5 (C-20, sc-1974; Santa Cruz Biotechnology), or γ-H2AX (05-636; Millipore).

Characterization of MEFs and splenocytes. Mouse embryonic fibroblasts (MEFs) were isolated from embryonic day 13.5 (E13.5) embryos and cultured using standard protocols (29). Immortalization was achieved by retroviral infection with a plasmid encoding the first 121 amino acids of the simian virus 40 (SV40) large T antigen (T121) following hygromycin selection. To induce Aurkb expression, doxycycline was added at a final concentration of 1 μg/μl (D-9891; Sigma-Aldrich). For growth curve assays, 50,000 cells were plated in triplicate and were treated with doxycycline or left untreated. The number of cells was counted on a daily basis for a week of treatment. The following drugs were used in cultured cells at the indicated concentrations: nocodazole (3.5 μM; Sigma), paclitaxel (originally named taxol; 1 μM [Sigma]), reversine (1 μM; Sigma), and ZM447439 (2 μM; Tocris Bioscience). To induce DNA damage, immortal murine MEFs were treated with doxycycline for 24 h and 1 μM doxorubicin (Adriamycin) was then added for 2 h, and samples were taken 6 and 10 h later. For DNA damage *in vivo*, $Aurkb^{+/+}$; $Rosa26^{M2rtTA/M2rtTA}$ and $Aurkb^{+/tet}$ $Rosa26^{M2rtTA/M2rtTA}$ mice were treated for 15 days with doxycycline and exposed to a single dose of 8 Gy of gamma radiation. For time-lapse imaging experiments, synchronous, histone H2B-green fluorescent protein (GFP)-expressing cells were recorded (5-min frames for 24 h) using a DeltaVision RT imaging system (Applied Precision, LLC; Olympus IX70/71 microscope) equipped with a charge-coupled-device camera (CoolSNAP HQ; Roper Scientific). Images were analyzed using ImageJ software (National Institutes of Health, Bethesda, MD, USA [http://rsb.info.nih.gov]).

Splenocytes were isolated and stimulated to enter cell cycle by culturing them in RPMI medium with the addition of concanavalin A (ConA) (3 μg/ml; Sigma) and lipopolysaccharide (LPS) (1 μg/ml; Sigma) for 96 h. For DNA content analysis, cells were stained with 5-ethynyl-2′-deoxyuridine (EdU) (10 μM; Sigma) for 30 min and then fixed in 70% ethanol overnight at −20°C. The following day, 4′,6′-diamidino-2-phenylindole (DAPI) (2 μg/ml; Sigma) was added, and cells were analyzed by flow cytometry (Becton Dickinson). FlowJO software was used to analyze cell populations.

Real-time PCR. Total RNA from cells and tissues was isolated using TRIzol (Invitrogen). Expression of Aurora B was quantified by real-time quantitative amplification with a SuperScript III Platinum assay kit, according to the manufacturer's instructions, in a Bio-Rad iCycler Real-Time PCR apparatus. The following primers were used: Aurkb forward (FW), 5′-AGGTCTGCAGGGAGAACTGA-3′; Aurkb reverse (RV), 5′-AGGCACAGAAGAGGGGAACT-3′; p21 FW, 5′-CTAGGGGAATTGGAGTCAGGC-3′; and p21 RV, 5′-AACAGGTCGGACATCACCAG-3′. Amplification of anti-glyceraldehyde-3-phosphate dehydrogenase (anti-GAPDH) was used for normalization using the following oligonucleotides: GAPDH FW, 5′-GCCACCCAGAAGACTGTGGATGGC-3′; GAPDH RV, 5′-CATGATGGCCATGAGGTCCACCAC-3′. Data analysis was performed using iQ5, version 2.0, software (Bio-Rad).

Immunofluorescence and protein analysis. The protocol for immunofluorescence in cultured cells was adapted from Perera et al. (30). Cells grown in coverslips were incubated overnight at 4°C in a humid chamber with human anticentromere antibodies (ACA) (1:500; Antibodies, Inc.) or primary antibodies against α-tubulin (Tub2.1, 1:250; Sigma-Aldrich), Aurora B (ab2254, 1:250; Abcam), BubR1 (SBR1.1, 1:100; a gift from S. S. Taylor), Mad2 (1:200; gift of K. Wassmann), phosphorylated Hec1 (phospho-S55, 1:200; GeneText), or phospho-histone H3 Ser10 (P-H3, 1:500; Upstate Biotechnologies). Matching secondary antibodies (Alexa 488 or 594) were from Molecular Probes (Invitrogen). Images were acquired using a Leica D3000 microscope or a Leica TCS-SP5-AOBS-UV confocal ultraspectral microscope.

For immunoblotting, cells or tissues were harvested and lysed in Laemmli buffer supplemented with protease and phosphatase inhibitor cocktails (Sigma), and 50 μg of total protein was separated by SDS-PAGE and probed with antibodies against Aurora B (ab2254, 1:200; Abcam), phospho-H2AX (Ser139) (05-636, 1:1,000; Millipore), $p21^{Cip1}$ (sc-397, 1:1,000; Santa Cruz Biotechnology), p53 (1:500) (2524, clone 1C12; Cell Signaling), β-actin (A4700, 1:2,000; Sigma-Aldrich), α-tubulin (T7451, 1:1,000; Sigma-Aldrich), or vinculin (V9131, 1:2,000; Sigma-Aldrich).

Karyotyping and scoring of aneuploidy. Cultured cells were exposed to colcemid for 5 h and hypotonically swollen in 40% full medium–60% tap water for 5.5 min. Hypotonic treatment was stopped by addition of an equal volume of Carnoy's solution (75% pure methanol, 25% glacial acetic acid); cells were then spun down and fixed with Carnoy's solution for 10 min. After fixation, cells were dropped from a 5-cm height onto glass slides previously treated with 45% acetic acid. Slides were mounted with ProLong Gold antifade reagent with 4,6-diamidino-2-phenylindole (DAPI; Invitrogen), and images were acquired with a Leica D3000 microscope and a 60 PlanApo N (numerical aperture [NA],1.42) objective. Chromosomes from 50 cells per genotype were counted using ImageJ software. Blood lymphocytes were extracted using Lymphocyte-M cell separation medium (Cedarlane), and cytospin preparations from these samples (interphasic lymphocytes) were analyzed by chromosome fluorescence *in situ* hybridization (FISH). Probes from two mouse bacterial artificial chromosome (BAC) clones (a gift from A. Losada, CNIO) of chromosome 8 (RP23-310L10) and chromosome 11 (RP23-263C13; both a gift of R. Sotillo and R. Benezra) were labeled with Spectrum Green-dUTP and Spectrum Red-dUTP (Vysis), respectively. The BAC DNAs were labeled by nick translation (Abbot, Inc.) according to standard protocols. The number of hybridization signals for these probes was assessed in a minimum of 100 interphase nuclei with well-delineated contours. Cells with only one probe signal were not considered.

Statistical and imaging analysis. Statistical analysis was performed using Student's *t* test, Fisher's exact test, or log rank tests (GraphPad Prism, version 5). All data are shown as means ± standard deviations (SD). Probabilities (*P*) of <0.05 or alpha values of <0.05 (Fisher's exact test) were considered significant. Images were quantified using ImageJ. Expression data in human tumors was obtained from the Gene Expression Omnibus (GEO) database (accession number GSE11877) (31, 32) and analyzed using GraphPad Prism, version 5.

RESULTS

Generation and characterization of an endogenous Aurora B-inducible model. To generate a model with inducible expression of Aurora B, we genetically modified the promoter region of the corresponding murine gene (*Aurkb*) (Fig. 1a). Specifically, we replaced 2 kb upstream of the translation initiation codon ATG by a tetracycline-responsive minimal promoter (27). Clones in which homologous recombination occurred were selected by Southern blotting (Fig. 1b). These clones were aggregated into developing blastocysts to generate $Aurkb^{+/lox\text{-}tet}$ mice. The puromycin resistance cassette was then removed by crossing the mice with transgenic mice expressing the Cre recombinase (33) resulting in the $Aurkb^{+/tet}$ mice (Fig. 1a). We were not able to obtain homozygous $Aurkb^{lox\text{-}tet/lox\text{-}tet}$ or $Aurkb^{tet/tet}$ mutants from crosses between heterozygous mice, in agreement with a lethal phenotype caused by the lack of Aurora B in embryos (34).

To generate an inducible system, these alleles were introduced

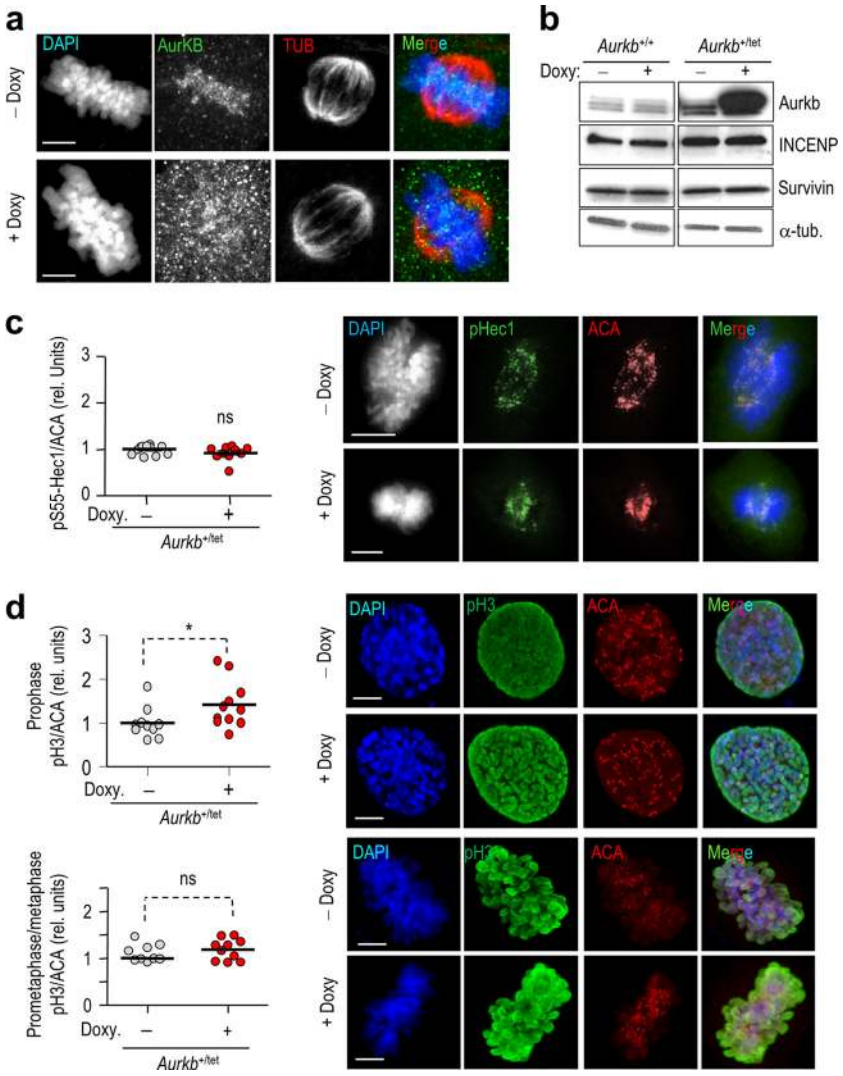

FIG 2 Localization and activity of overexpressed Aurora B. (a) Detection of Aurora B (green in the merged image) by immunofluorescence in the absence or presence of doxycycline. Data are representative of 50 mitotic cells analyzed per condition. Scale bars, 10 μm. (b) Protein levels of the CPC components in Aurora B-overexpressing and control MEFs. α-Tubulin was used as a loading control. (c) Phosphorylation of Hec1 (phospho-S55; pHec1) in prometaphase Aurora B-overexpressing cells. rel, relative. (d) Phosphorylation of histone H3 (pH3) in prophase or prometaphase/metaphase Aurora B-overexpressing cells. In panels a, c, and d, DAPI (blue) was used to stain DNA, and anticentromere antigen (ACA; red) was used as a control of centromeric localization. In panels c and d, horizontal bars indicate means ($n = 10$ to 12 mitotic cells per condition). ns, not significant; *, $P = 0.05$ (Student's t test).

into mice expressing an M2rtTA transactivator under the ubiquitous Rosa26 promoter (28). *Aurkb*$^{+/tet}$; *Rosa26*$^{M2rtTA/M2rtTA}$ and *Aurkb*$^{+/lox\text{-}tet}$; *Rosa26*$^{M2rtTA/M2rtTA}$ mouse embryonic fibroblasts (MEFs) were obtained and cultured in the absence or presence of doxycycline. Treatment with doxycycline induced a significant increase in Aurora B mRNA (Fig. 1c) and protein (Fig. 1d) levels. Aurora B was always induced to a higher level in *Aurkb*$^{+/tet}$ than in *Aurkb*$^{+/lox\text{-}tet}$ MEFs, and we therefore selected *Aurkb*$^{+/tet}$ clones for further assays. Induction of Aurora B was also evident in serum-starved MEFs (Fig. 1e) and noncycling lymphocytes (Fig. 1f and g) treated with doxycycline, indicating that Aurora B gene induction in this system is independent of cell cycle regulation. In these assays, treatment with doxycycline resulted in a significant increase in the intracellular levels of Aurora B, which displayed a pancellular localization in mitosis in addition to the normal centromeric localization (Fig. 2a). Overexpression of Aurora B did not significantly affect the levels of its CPC partners INCENP or survivin (Fig. 2b). In addition, we did not observe a significant increase in the levels of Hec1 phosphorylation (Fig. 2c, pHec1). Similarly, phosphorylation of histone H3 was not increased in prometaphase or metaphase although it was slightly increased in prophase (Fig. 2d, pH3).

Aurora B overexpression results in mitotic defects and aneuploidy. Treatment of *Aurkb*$^{+/tet}$; *Rosa26*$^{M2rtTA/M2rtTA}$ MEFs with doxycycline for 6 days resulted in impaired proliferation compared to that in untreated *Aurkb*$^{+/tet}$ clones or control *Aurkb*$^{+/+}$ fibroblasts (Fig. 3a). The proliferation of untreated *Aurkb*$^{+/tet}$ MEFs was reduced compared to that of wild-type cells probably as a consequence of the presence of a single functional *Aurkb* allele in these mutant cells. Overexpression of Aurora B did not significantly alter the percentage of cells in mitosis although these mutant cells displayed an increased percentage of prometaphase cells

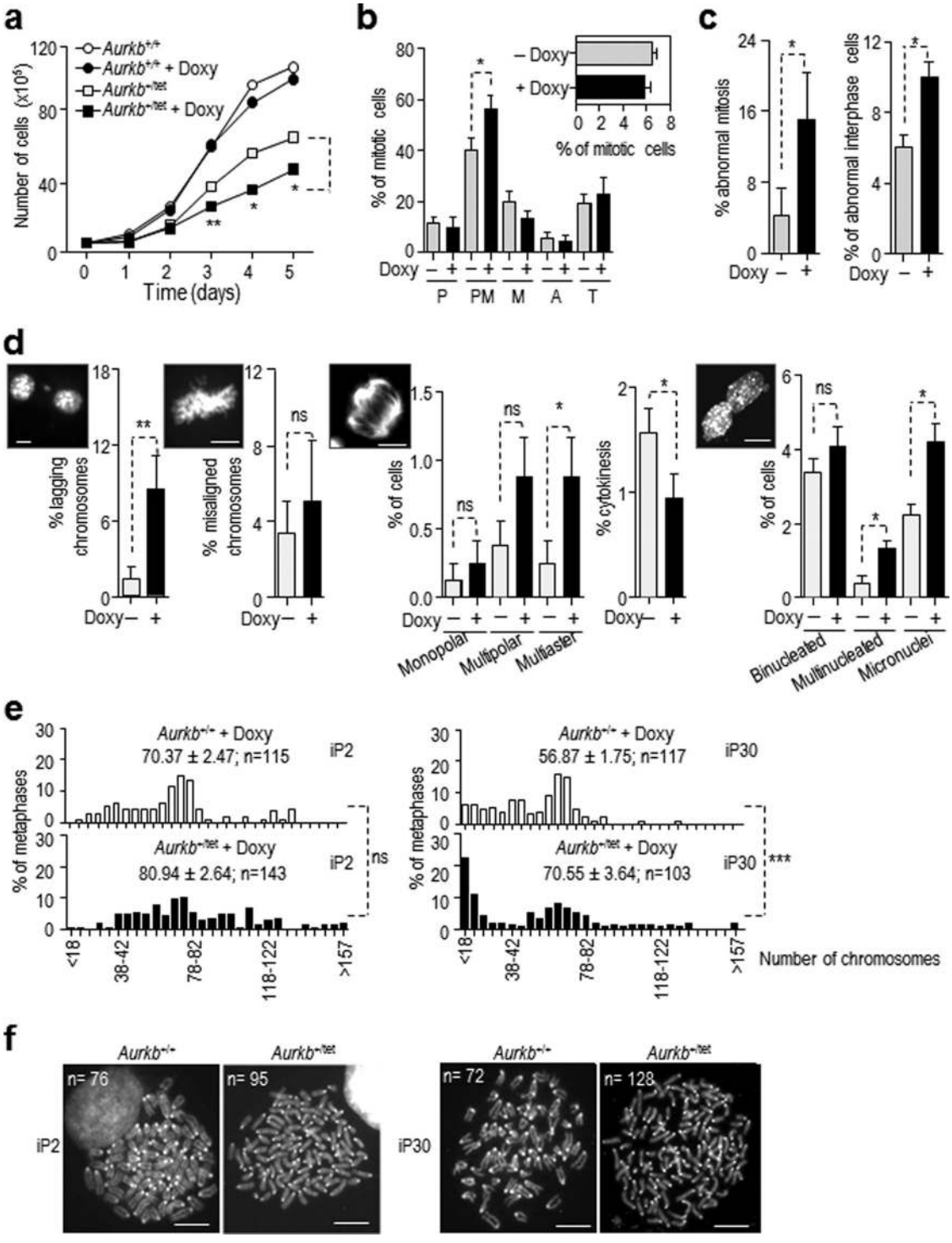

FIG 3 Overexpression of Aurora B results in chromosome segregation defects. (a) Proliferation of early-passage primary MEFs with or without the addition of doxycycline. *Aurkb*$^{+/+}$ and *Aurkb*$^{+/tet}$ cells (always in the presence of the *Rosa26*^{M2rtTA} allele) were treated with doxycycline or left untreated for 5 days. Data are representative of two different clones per condition. (b) Percentage and distribution of mitotic cells indicating the percentage of prometaphase (PM), metaphase (M), anaphase (A), or telophase (T) cells 48 h after the addition of doxycycline ($n = 400$ cells per treatment). (c) Percentage of abnormal mitotic figures (left panel) or abnormal interphasic cells (right panel) (bi-, multi-, and micronucleated cells; as shown in panel d) in *Aurkb*-overexpressing cells ($n = 50$ cells per treatment). (d) Percentage of mitotic defects (lagging or misaligned chromosomes and aberrant spindles), cytokinesis figures, and nuclear alterations in interphase in *Aurkb*$^{+/tet}$ MEFS in the absence or presence of doxycycline. Representative pictures are shown in the upper parts of the graphs. DAPI was used to stain DNA. Scale bars, 5 μm. $n = 400$ cells per condition. (e) Cytogenetic analysis of immortalized MEFs after exposure to 5 h of colcemid. The absolute numbers of chromosomes per metaphase were grouped in categories at early (passage 2) or late (passage 30) immortal passages (iP2 or iP30, respectively). Data are means ± standard deviations. *n*, number of metaphases analyzed per genotype. (f) Representative images of chromosome spreads from the indicated cultures. *n*, number of chromosomes per metaphase. ns, not significant; *, $P < 0.05$; **, $P < 0.01$; ***, $P < 0.001$ (Student's *t* test).

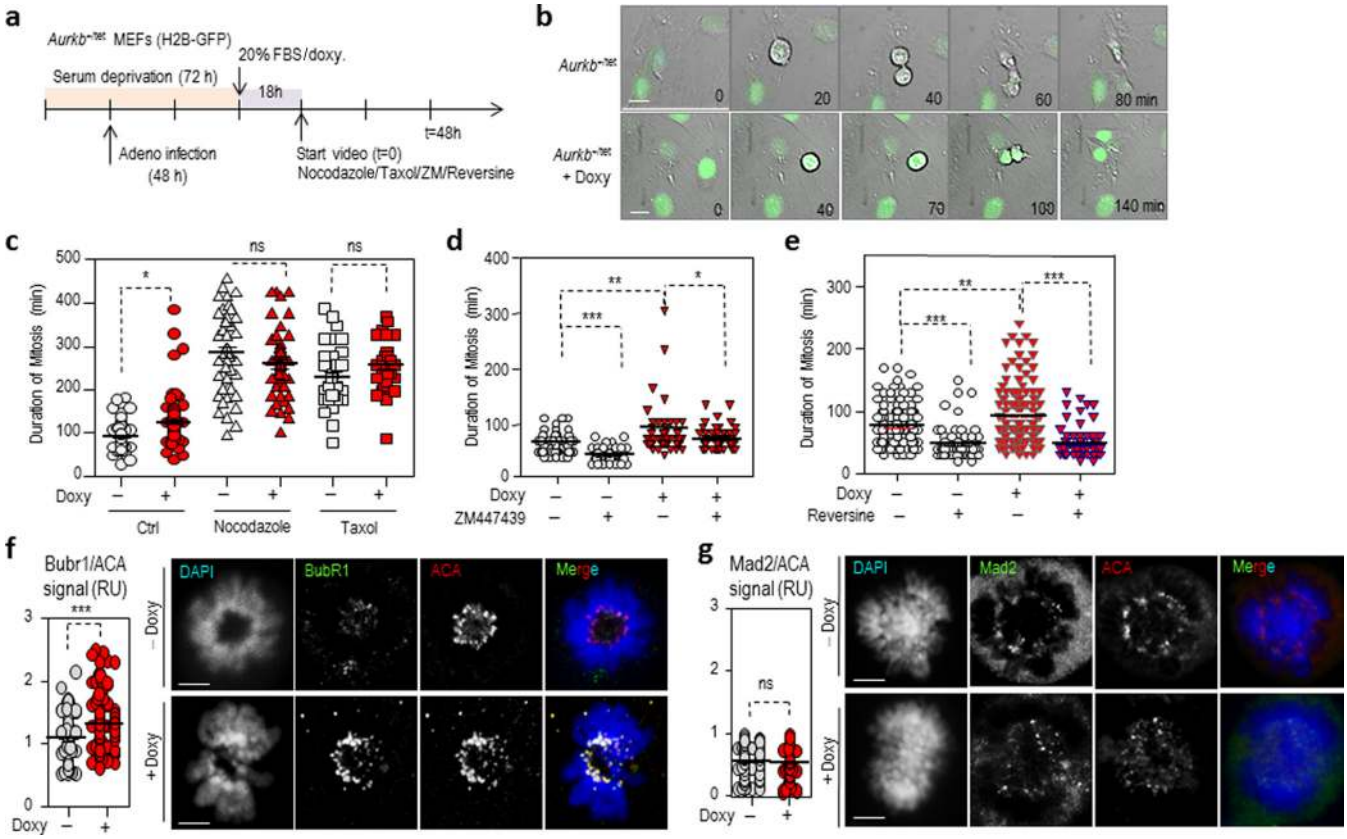

FIG 4 Overexpression of Aurora B results in increased duration of mitosis accompanied by enhanced kinetochore loading of BubR1. (a) Schematic representation of the protocol used for time-lapse microscopy. Confluent cultures of immortalized *Aurkb*$^{+/tet}$; *Rosa26*$^{M2rtTA/M2rtTA}$ MEFs were infected with adenoviruses (Adeno) expressing GFP-tagged histone H2B (H2B-GFP) following serum deprivation for 48 h. These cells were stimulated with serum and treated or not treated with doxycycline for 18 h. Then, the cells were left untreated or exposed to different drugs; next, they were monitored by using time-lapse microscopy during an additional 48 h. (b) Representative images of the indicated cultures during mitosis. The numbers of cells analyzed is indicated in each frame. Scale bars, 10 μm. H2B-GFP is in green. (c) Duration of mitosis in immortal untreated *Aurkb*$^{+/tet}$ ($n = 74$ cells) or doxycycline-induced *Aurkb*$^{+/tet}$ ($n = 82$ cells) MEFs showing an increase in the duration of mitosis when cells overexpress Aurora B. No differences were found when cells were exposed to 3.5 μM nocodazole or 1 μM paclitaxel. (d) The delay in mitotic exit upon Aurora B overexpression was rescued by the Aurora B inhibitor ZM447439 ($n = 49$ to 60 cells per condition). (e) The delay in mitotic exit upon Aurora B overexpression was rescued by the Mps1 inhibitor reversine ($n = 65$ to 100 cells per condition). Ratio between BubR1 (f) and Mad2 (g) to anticentromere antigen (ACA) signal in *Aurkb*$^{+/tet}$ MEFs treated or not treated with doxycycline ($n =$ at least 70 centromere signals per group). Representative images of BubR1 and Mad2 (green) staining at kinetochores in untreated or doxycycline-treated *Aurkb*$^{+/tet}$ MEFs are also shown. ACA is shown in red, and DNA (DAPI) is in blue. Three different clones from each genotype/condition were analyzed. RU, relative units. Scale bars, 10 μm. ns, not significant; *, $P < 0.05$; **, $P < 0.01$; ***, $P < 0.001$ (Student's *t* test). Horizontal bars indicate means.

(40.3% ± 4.6% versus 56.3% ± 5.4%; $P = 0.02$) (Fig. 3b). Mitotic defects, mostly lagging chromosomes and spindles with multiple asters, were significantly more abundant in *Aurkb*$^{+/tet}$ cells treated with doxycycline (14.4% ± 3.7% versus 4.8% ± 2.7% in untreated cells; $P = 0.0245$) (Fig. 3c and d). The percentage of aberrant interphase cells, including multinucleated cells or cells with micronuclei, was also more frequent upon Aurora B overexpression (9.8% ± 1.9% versus 6.3% ± 0.7% in control cultures; $P = 0.0489$) (Fig. 3c and d).

In order to assess whether Aurora B overexpression induced chromosomal instability, we performed karyotype analyses of metaphase spreads generated from early (passage 2) or late (passage 30) immortal MEFs. As shown in Fig. 3e, overexpression or Aurora B in early-passage cells resulted in a broader variance in the number of chromosomes after 5 days in doxycycline. In addition, whereas control cultures were relatively stable 30 passages later, Aurora B-overexpressing cells showed a significantly wider variance in their chromosome numbers (Fig. 3e and f), as expected from the missegregation of chromosomes during cell division.

Aurora B is involved in the error correction mechanism that monitors chromosome attachments to the spindle, and its activity generates unattached kinetochores that are sensed by the spindle assembly checkpoint (SAC). We therefore analyzed mitotic progression in Aurora B-overexpressing and control cells (Fig. 4a). Whereas overexpression of Aurora B did not alter the response to microtubule poisons such as paclitaxel or nocodazole in MEFs, the duration of mitosis was increased in Aurora B-overexpressing MEFs in the absence of these microtubule poisons (137.7 ± 9.7 min versus 108.2 ± 5.5 in untreated *Aurkb*$^{+/tet}$ cells) (Fig. 4b and c). This defect was prevented by treatment of Aurora B-overexpressing cells with the Aurora B inhibitor ZM447439 (Fig. 4d), which had no obvious effect on Plk1 or Cdk1 kinase activity (data not shown). In addition, the defect in the duration of mitosis was rescued by the Mps1 inhibitor reversine (Fig. 4e), suggesting that mitotic delay in the presence of increased Aurora B levels was caused by SAC activation. Whereas we found no significant differences in the loading of BubR1 or Mad2 to kinetochores in the presence of microtubule poisons (data not shown), we observed a

significant increase in BubR1 protein levels at centromeres in unperturbed *Aurkb*$^{+/tet}$ MEFs overexpressing Aurora B (Fig. 4f). Levels of centromeric Mad2, however, were unaffected in these cells (Fig. 4g), suggesting a specific limiting role for Aurora B in the kinetochore localization of BubR1.

Aurora B suppresses the expression of the cell cycle inhibitor p21^{Cip1}. Aurora B has been shown to inactivate p53 function, lowering expression of its target genes *in vitro* (24, 25). We therefore explored whether p53 or its target genes were affected by Aurora B overexpression in cells treated with the topoisomerase II inhibitor doxorubicin (Fig. 5a). The doxycycline-dependent induction of Aurora B correlated in these cells with a significant reduction in the level of induction of p21^{Cip1} transcripts (Fig. 5b) and protein (Fig. 5c). In these assays, the levels of p53 were significantly increased with doxorubicin but were not affected by Aurora B overexpression (Fig. 5c). On the contrary, phosphorylation of p53 at Ser15 was decreased in these Aurora B-overexpressing cells (Fig. 5c), suggesting that Aurora B affects p53 activity rather than protein levels.

We next analyzed whether Aurora B regulates the p53 pathway *in vivo* by treating *Aurkb*$^{+/+}$ and *Aurkb*$^{+/tet}$ mice, in the presence of the *Rosa26*$^{M2rtTA/M2rtTA}$ alleles, with gamma irradiation (8 Gy). The intensity of Aurora B immunostaining increased in the white pulp of the spleen after treatment with doxycycline in both irradiated and nonirradiated mice (Fig. 5d). Whereas overexpression of Aurora B did not significantly alter the induction of p53 in these irradiated mice, the percentage of p21^{Cip1}-positive cells was significantly reduced in irradiated *Aurkb*$^{+/tet}$ mice compared to that in wild-type controls (Fig. 5d). This effect was accompanied by a reduced response to DNA damage, as scored by phosphorylation of H2AX (γH2AX), and a significant decrease in the ratio of apoptotic cells after irradiation (Fig. 5d), suggesting that overexpression of Aurora B impairs the DNA damage response *in vivo*.

Aurora B-overexpressing mice are tumor prone. To monitor long-term effects of Aurora B overexpression *in vivo*, *Rosa26*$^{M2rtTA/M2rtTA}$ mice harboring the mutant *Aurkb*^{tet} or *Aurkb*$^{lox\text{-}tet}$ allele were treated with doxycycline in the drinking water for 20 months. We first confirmed the *in vivo* induction of Aurora B by analyzing mRNA (Fig. 6a) and protein levels (Fig. 6b and c) in several proliferative and nonproliferative tissues. Although both mutant alleles resulted in Aurora B overexpression, the levels of Aurora B were higher in *Aurkb*$^{+/tet}$ tissues than in the corresponding *Aurkb*$^{+/lox\text{-}tet}$ samples.

We next asked whether overexpression of Aurora B caused aneuploidy in peripheral blood lymphocytes of mutant mice by scoring interphase nuclei by fluorescence *in situ* hybridization (FISH) using probes against chromosomes 8 and 11. Age-dependent accumulation of aneuploidy in lymphocytes was observed in mice of both genotypes although *Aurkb*$^{+/tet}$ animals contained a significantly higher percentage of aneuploid cells (Fig. 6d). The percentage of aneuploidy, calculated as the deviation from the mode, was 0.28% in 4-month-old *Aurkb*$^{+/+}$ mice and 3.04% in *Aurkb*$^{+/tet}$ littermates ($P = 0.0021$). At 20 months of age, these numbers increased to 3.00% in *Aurkb*$^{+/+}$ and 7.66% in *Aurkb*$^{+/tet}$ mice ($P = 0.0033$) (Fig. 6d and e). Levels of aneuploidy were not significantly different when untreated *Aurkb*$^{+/+}$, *Aurkb*$^{+/lox\text{-}tet}$, or *Aurkb*$^{+/tet}$ mice aged 20 months were analyzed (data not shown).

Importantly, *Aurkb*$^{+/tet}$ and *Aurkb*$^{+/lox\text{-}tet}$ mice were characterized by a high incidence of tumor development during ageing. Whereas spontaneous tumors were detected in 14.3% of control mice, 58.3% of the *Aurkb*$^{+/lox\text{-}tet}$ mice and more than 90% of the *Aurkb*$^{+/tet}$ mice had at least one tumor ($P = 0.0006$, for *Aurkb*$^{+/tet}$ versus wild-type mice) (Fig. 7a). Furthermore, 60% of *Aurkb*$^{+/tet}$ mice and 25% of *Aurkb*$^{+/lox\text{-}tet}$ mice were simultaneously affected with more than one tumor type. Histological analysis of both *Aurkb*$^{+/tet}$ and *Aurkb*$^{+/lox\text{-}tet}$ mice showed a wide spectrum of tumors, with spleen lymphomas being the most common neoplasia (25% and 93.3% of *Aurkb*$^{+/lox\text{-}tet}$ and *Aurkb*$^{+/tet}$ mice, respectively) (Fig. 7a). These lymphomas were follicular B-cell subtype (Pax5-positive), characterized by enlarged spleen follicles populated by a mixture of cells, including centrocytes, centroblasts, and Cd3^{+} T cells (Fig. 7b and c). *Aurkb*$^{+/tet}$ lymphomas presented a higher degree of aggressiveness, as shown by infiltrations in the lung, liver, kidney, and bone marrow, where these tumors preferentially metastasized (Fig. 7d). Aurora B overexpression in *Aurkb*$^{+/tet}$ mice also resulted in sarcomas (25%), alveolar type II cell adenomas in the lung (13.33%), and liver hemangiomas (20%) as well as other more infrequent tumors and nontumoral lesions (Fig. 7b).

Aurora B-overexpressing tumors display increased aneuploidy and reduced p21^{Cip1} levels. Spleen sections from tumor-bearing and healthy 20-month-old *Aurkb*$^{+/tet}$ and wild-type mice were hybridized with FISH probes against chromosomes 8 and 11. The percentage of aneuploid cells in small, nonmetastatic (initial) or advanced, metastatic *Aurkb*$^{+/tet}$ tumors was significantly higher than that in nontumoral (NT) spleen cells from age-matched wild-type animals (Fig. 8a). Aneuploidy also increased in the spontaneous tumors observed in *Aurkb*$^{+/+}$ mice (8% aneuploid cells) although it never reached the levels found in initial (10.9%) or advanced (14.8%) *Aurkb*$^{+/tet}$ tumors. This increase in total aneuploidy reflected an increase in both near-diploid and near-tetraploid aneuploid cells within spleen lymphomas (Fig. 8b). Similar results were found in lung tumors, the most prominent epithelium-originating tumor in *Aurkb*$^{+/tet}$ mice, which reached 17.5% aneuploid cells (data not shown). Together, these data suggest that Aurora B overexpression leads to chromosomal instability *in vivo*, which may proceed to overt transformation.

Since Aurora B can modulate p21^{Cip1} levels (Fig. 5), we also analyzed p53 and p21^{Cip1} levels in spleen tumors. p53 protein levels were significantly reduced in *Aurkb*$^{+/tet}$ tumors in comparison to levels in tumoral or nontumoral spleen samples from *Aurkb*$^{+/+}$ mice (Fig. 8c). Similarly, a significant decrease in p21^{Cip1} levels was also found in spleen tumors from *Aurkb*$^{+/tet}$ mice compared with levels in similar tumors from *Aurkb*$^{+/+}$ animals (Fig. 8d). p21^{Cip1} was almost absent in metastatic *Aurkb*$^{+/tet}$ tumors, in line with their aggressive phenotype. To test whether these observations might also apply to human lymphoblastic leukemias, we compared *AURKB* and *CDKN1A* (the human gene encoding p21^{Cip1}) mRNA levels in B-cell acute lymphoblastic leukemia (B-ALL) samples (31, 32). As represented in Fig. 8e, the levels of expression of these transcripts displayed a significant inverse correlation in which p21^{Cip1} expression was constantly low in tumors expressing high levels of Aurora B. All together, these data suggest that Aurora B overexpression triggers tumor development *in vivo* in association with both increased aneuploidy and defective p21^{Cip1} function.

DISCUSSION

Aurora B, the catalytic component of the chromosomal passenger complex (CPC), is an essential kinase in the error correction

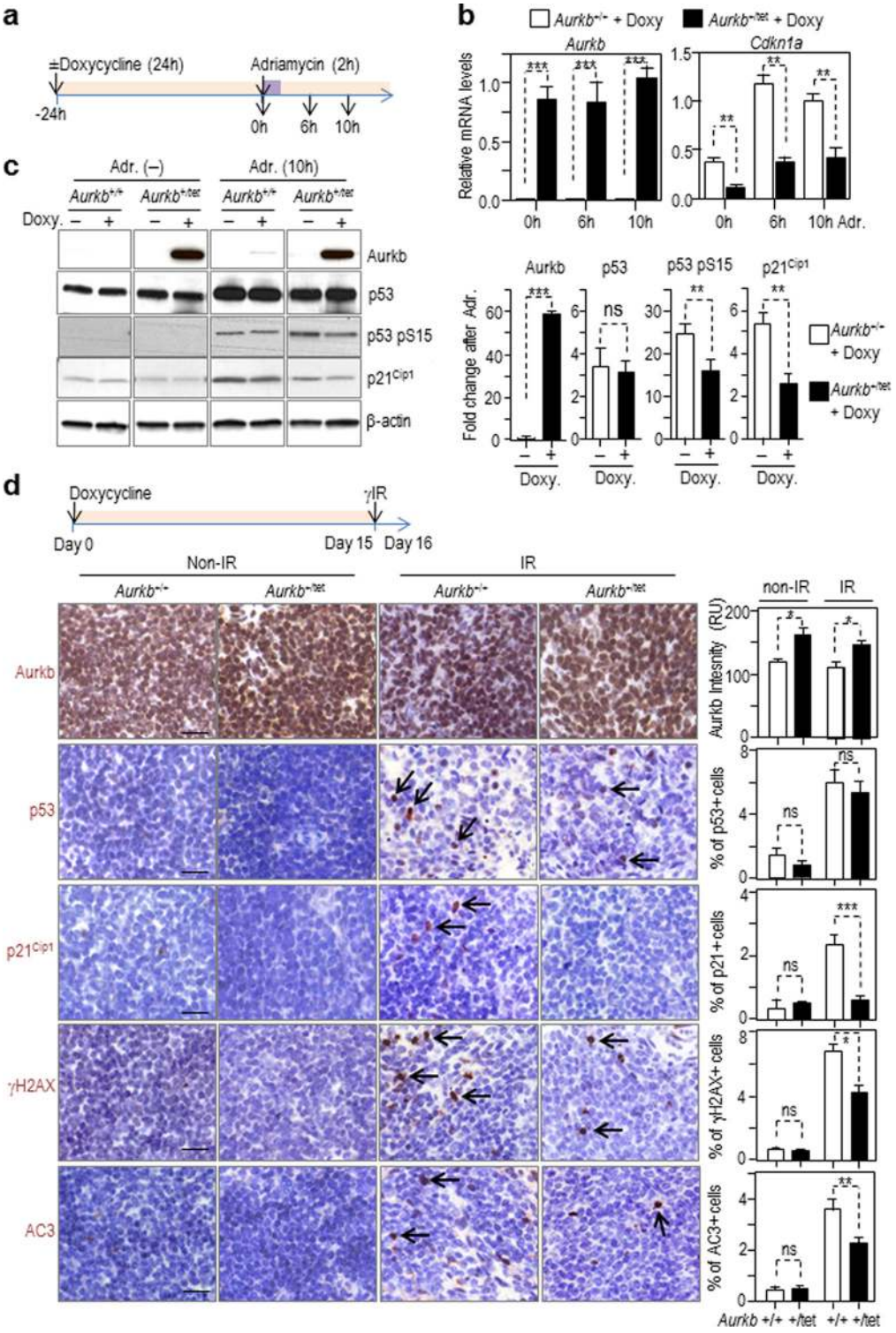

FIG 5 Overexpression of Aurora B impairs the DNA damage response. (a) Schematic representation of the DNA damage assay performed in *Aurkb*$^{+/tet}$; *Rosa26*$^{M2rtTA/M2rtTA}$ and *Aurkb*$^{+/+}$; *Rosa26*$^{M2rtTA/M2rtTA}$ MEFs. Cells were treated with doxycycline (Doxy) for 24 h and doxorubicin (Adriamycin, Adr) was added for 2 h in order to induce p53 signaling. The protein levels of the indicated proteins were assessed before or at 10 h post-damage induction, and the fold change versus that in nondamaged cells is shown in the right histograms. (b) mRNA levels of *Aurkb* and *Cdkn1a* (encoding p21^{Cip1}) transcripts in doxycycline-treated *Aurkb*$^{+/tet}$; *Rosa26*$^{M2rtTA/M2rtTA}$ and *Aurkb*$^{+/+}$; *Rosa26*$^{M2rtTA/M2rtTA}$ MEFs at the indicated times (0, 6, or 10 h) after treatment with doxorubicin (Adriamycin, Adr). GAPDH transcripts were used for normalization. Data are representative of three experiments. (c) Levels of the indicated antigens in the absence (−) or presence (10 h) of doxorubicin (Adriamycin, Adr) treatment and/or doxycycline (Doxy). The histogram shows the means ± standard deviations ($n = 4$ independent assays) of the change of these protein levels upon doxorubicin treatment in control or *Aurkb*$^{+/tet}$ cells treated with doxycycline. (d) To induce DNA damage *in vivo*, 6- to 8-week-old *Aurkb*$^{+/+}$; *Rosa26*$^{M2rtTA/M2rtTA}$ (+/+ mice) and *Aurkb*$^{+/tet}$; *Rosa26*$^{M2rtTA/M2rtTA}$ (+/*tet*) mice were treated for 15 days with doxycycline and irradiated (IR; 8 Gy of gamma irradiation). Cells positive for the corresponding antigens are indicated by arrows. The levels of the indicated proteins were tested by immunohistochemistry in the spleen 24 h later. γH2AX, phosphorylated H2AX; AC3, active caspase 3. Scale bars, 50 μm. Data in the histograms indicate means ± standard deviations. At least 15,000 cells were counted per genotype and condition ($n = 4$ irradiated and 2 nonirradiated mice). ns, not significant; *, $P < 0.05$; **, $P < 0.01$; ***, $P < 0.001$ (Student's *t* test).

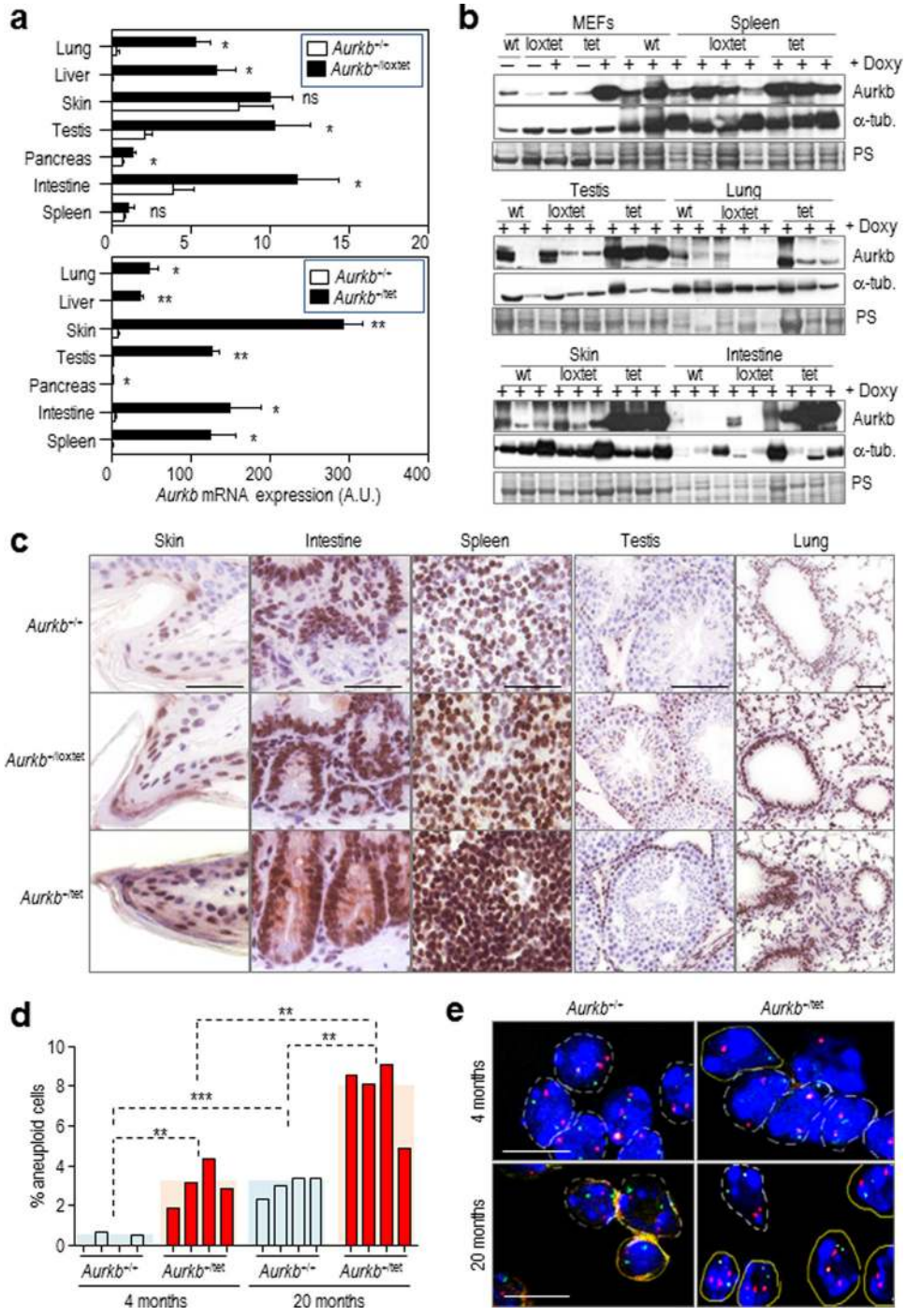

FIG 6 *In vivo* overexpression of Aurora B induces aneuploidy. (a) Expression of Aurora B transcripts in the indicated tissues from *Rosa26*$^{M2rtTA/M2rtTA}$ mice harboring the *Aurkb*$^{lox\text{-}tet}$ and *Aurkb*^{tet} alleles after treatment with doxycycline for 2 weeks. mRNA levels were normalized to the expression of *Gapdh* mRNA. Data are representative of three assays (2 mice per genotype). ns, not significant; *, $P < 0.05$; **, $P < 0.01$. (b) Immunodetection of Aurora B in MEFs of the indicated tissues from *Rosa26*$^{M2rtTA/M2rtTA}$ mice harboring the *Aurkb*$^{lox\text{-}tet}$ and *Aurkb*^{tet} alleles. α-Tubulin (α-tub) and Ponceau S (PS) were used as loading controls. wt, wild type. (c) Immunohistochemical detection of Aurora B for the indicated tissues and genotypes ($n = 3$ mice per condition). Scale bars, 50 μm. (d) Levels of aneuploid cells in *Aurkb*$^{+/+}$; *Rosa26*$^{M2rtTA/M2rtTA}$ and *Aurkb*$^{+/tet}$; *Rosa26*$^{M2rtTA/M2rtTA}$ mice after 4 or 20 months in the presence of doxycycline. Aneuploidy (deviation from the mode) was scored using FISH for two different chromosomes in lymphocytes from 4- and 20-month-old animals (at least $n = 100$ cells from each of four animals per genotype and time point). Each column represents one animal of the indicated genotype. **, $P < 0.01$; ***, $P < 0.001$ (Student's *t* test). (e) Representative images of interphasic FISH analysis using probes for chromosomes 8 (red) and 11 (green). At least 100 cells from each of four animals per genotype and time point were analyzed. Scale bars, 20 μm.

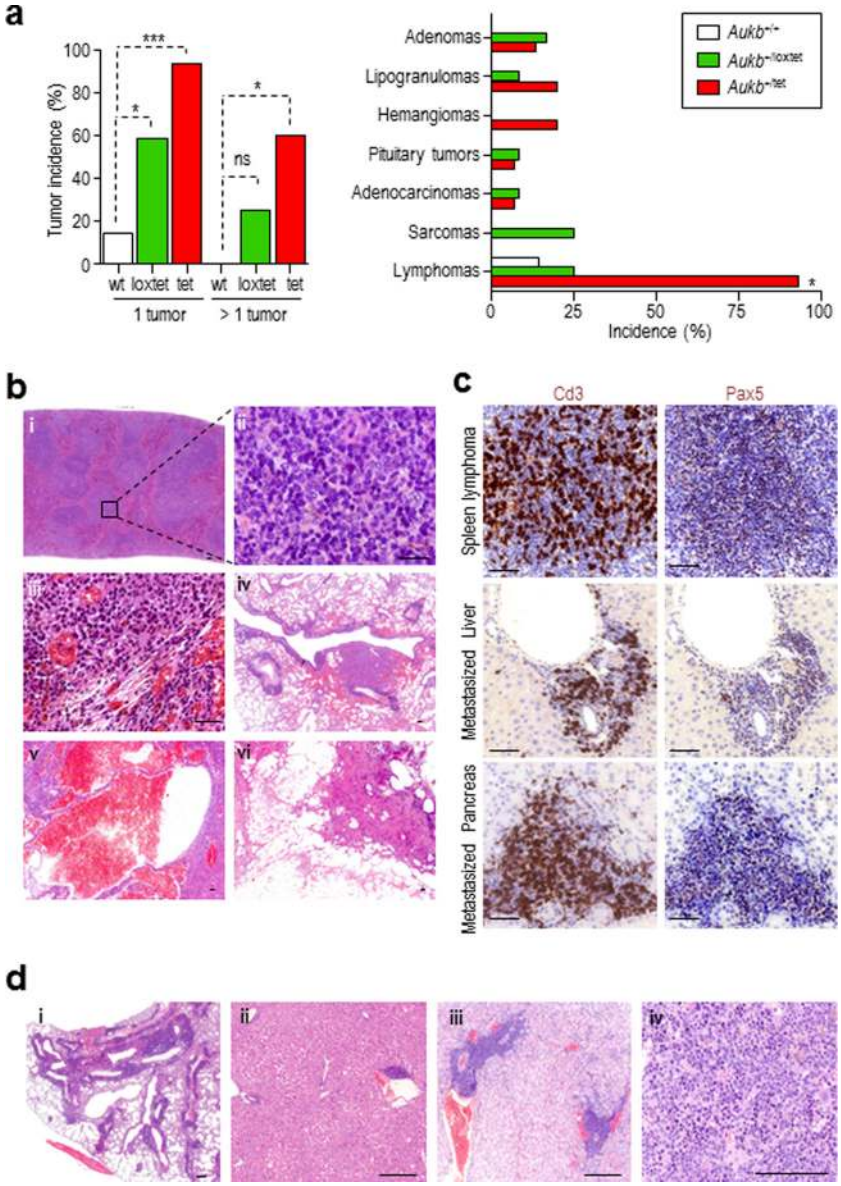

FIG 7 Tumor susceptibility in Aurora B-overexpressing mice. (a) Spontaneous tumor incidence (one tumor or more than one tumor per mouse) and type of neoplasias found in control ($n = 7$) or Aurora B-overexpressing ($n = 12$ $Aurkb^{lox\text{-}tet}$ and 15 $Aurkb^{tet}$) mice. ns, not significant; *, $P < 0.05$; ***, $P < 0.001$ (chi-square test). (b) Hematoxylin and eosin staining of the indicated tumors found in $Aurkb^{+/tet}$; $Rosa26^{M2rtTA/M2rtTA}$ mice. Frames i and ii, spleen lymphoma; frame iii, histiocytic sarcoma; frame iv, lung adenoma; frame v, liver hemangioma; frame vi, lipogranuloma. Scale bars, 100 μm. Frame ii is an enlargement of the boxed area in frame i. (c) Representative pictures of CD3 and Pax5 staining in tumor samples from the spleen, liver and pancreas of $Aurkb^{+/tet}$; $Rosa26^{M2rtTA/M2rtTA}$ mice. Scale bars, 50 μm. (d) Representative images of lymphoma metastasis in the lung (i), liver (ii), kidney (iii), and bone marrow (iv) in $Aurkb^{+/tet}$; $Rosa26^{M2rtTA/+}$ mice. Scale bars, 200 μm.

mechanism that ensures proper chromosome segregation when cells divide (8, 35). Reducing Aurora B activity by means of RNA interference or small-molecule inhibitors results in failure in chromosome alignment and defective kinetochore-microtubule attachment, cleavage furrow formation, and cytokinesis, ultimately leading to tetraploidization (36–39). Aurora B heterozygosity in the mouse results in increased tumor incidence, whereas complete loss of *Aurkb* prevents chromosome segregation and results in a premature mitotic exit (26, 34).

Although most studies have used loss-of-function approaches to understand the function of this kinase, Aurora B is overexpressed in many tumor types, and a correlation between its levels and tumor grade or poor clinical prognosis has been also proposed (16–18, 20–22). Previous cellular studies indicate that sustained overexpression of Aurora B in murine epithelial cells induces tetraploidy and chromosomal instability, increasing the oncogenic potential of cultured cells (12, 39, 40). A recent report in yeast cells suggests that these defects may be a consequence of the continuous disruption of chromosome-microtubule attachments even when sister chromatids are properly bioriented (11).

Here, we have taken advantage of a robust system to modulate the expression of endogenous genes in mammals by using a pro-

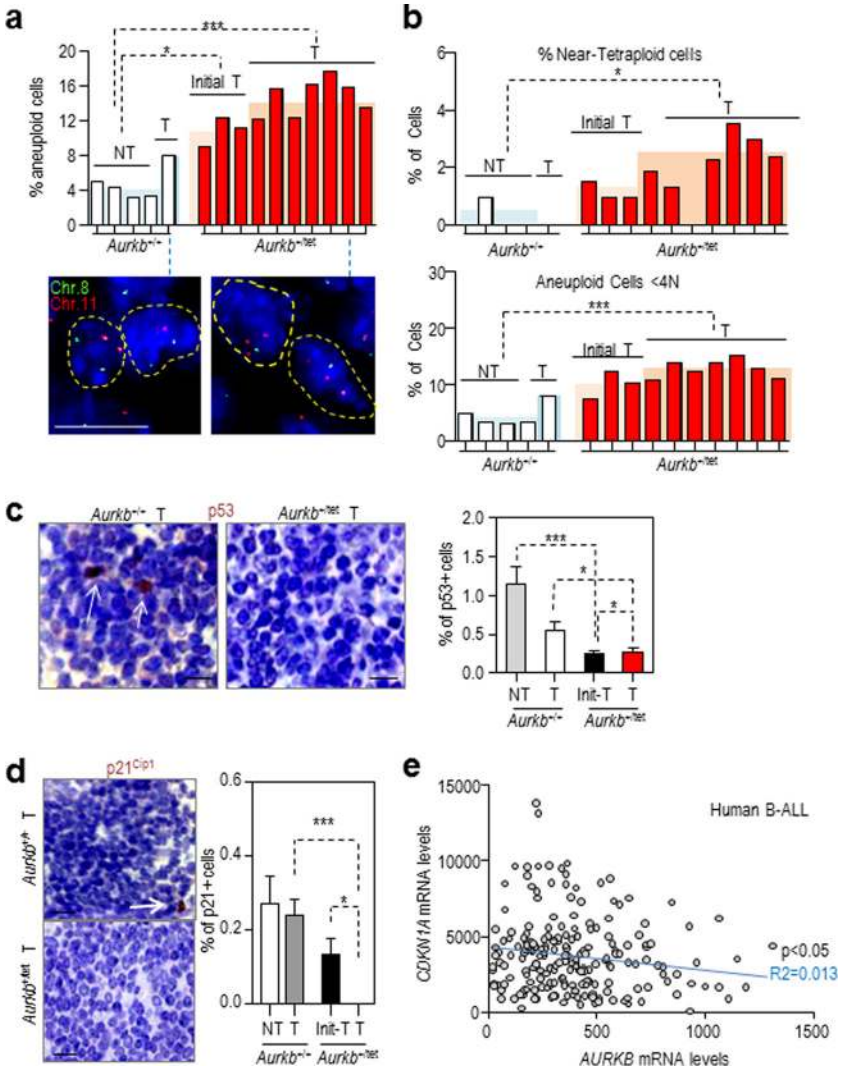

FIG 8 Aneuploidy and reduced $p21^{Cip1}$ levels in Aurora B-overexpressing tumors. (a) Percentage of aneuploid cells in nontumoral (NT) spleens or spleens with initial (small, nonmetastatic) or fully developed tumors (T) from the indicated genotypes. FISH was performed for chromosomes 8 (data not shown) and 11 (red in the image) on spleen sections from 80-week-old mice. Each column represents one animal of the indicated genotype. Representative images are shown at the bottom. DNA is shown in blue, and FISH probes to chromosome 8 and 11 are in green and red, respectively. Scale bar, 20 μm. At least 100 cells were counted per condition. (b) Percent of near-tetraploid cells and aneuploid cells (excluding those scored as near-tetraploid) determined by chromosome FISH hybridization in nontumoral (NT) or tumoral (either initial, Init-T or fully developed, T, tumors) spleen samples from *Aurkb*$^{+/+}$; *Rosa26*$^{M2rtTA/M2rtTA}$ and *Aurkb*$^{+/tet}$; *Rosa26*$^{M2rtTA/M2rtTA}$ mice. Each column represents one animal of the indicated genotype. At least 100 cells were counted per condition. (c) Immunodetection of p53 in nontumoral (NT) or tumoral (either initial or fully developed) spleen samples from *Aurkb*$^{+/+}$; *Rosa26*$^{M2rtTA/M2rtTA}$ and *Aurkb*$^{+/tet}$; *Rosa26*$^{M2rtTA/M2rtTA}$ mice. Scale bar, 80 μm. The quantification of the percentage of p53-positive cells (means ± standard deviations; $n > 10{,}000$ cells per genotype and condition) is shown in the histogram. (d) $p21^{Cip1}$ levels in nontumoral (NT) and tumoral (T) spleen samples from *Aurkb*$^{+/+}$ mice in comparison to levels in initial and fully developed tumors from *Aurkb*$^{+/tet}$ mice. Scale bar, 80 μm. The percentage of $p21^{Cip1}$-positive cells (means ± standard deviations; $n > 11{,}000$ cells per genotype and condition) is shown in the histogram. Significance in panels a to d is indicated as follows: *, $P < 0.05$; ***, $P < 0.001$ (Student's *t* test). (e) Inverse correlation between *AURKB* and *CDKN1A* mRNA levels in 207 samples of human B-cell acute lymphoblastic leukemia (B-ALL). Expression data obtained from Kang et al. and Harvey et al. (31, 32). Pearson correlation (R^2) and *P* values are indicated.

moter-hijack strategy previously used to modulate gene expression in chicken DT40 cells (27, 41). Replacement of endogenous promoter regions by tetracycline-responsive elements results in robust control of endogenous gene expression both *in vitro* and *in vivo*, eliminating the need to express exogenous genes (Fig. 1 and 5). The mouse model described here confirms the effect of Aurora B overexpression in the generation of misaligned chromosomes and in triggering an SAC-dependent response, as recently reported in yeast cells (11). These defects could be a consequence of kinetochore-microtubule attachment defects induced by saturated levels of the kinase at the kinetochores. Although we observed a slight increase in histone H3 S10 phosphorylation in prophase cells, we did not observe enhanced phosphorylation of mitotic Aurora B targets such as Hec1. Thus, our data are not conclusive to discriminate between kinase-dependent and -independent effects of Aurora B overexpression in these cells. Mitotic defects are accompanied by an increase in the length of mitosis and increased levels of BubR1 in kinetochores, in line with previ-

ous work showing that Aurora B participates in the recruitment of BubR1 but not Mad2 to kinetochores (34, 37).

Our ability to chronically induce Aurora B overexpression in the mouse allowed us to analyze the consequences of the resulting mitotic defects during ageing. Overexpression of Aurora B *in vivo* resulted in a significant increase in aneuploidy accompanied by a dramatic susceptibility to spontaneous tumors. The percentage of aneuploid cells in Aurora B-overexpressing normal or tumoral lymphocytes reached ~13 to 18%, similarly to previous models with Bub1 overexpression, although these levels are difficult to compare due to technical and biological reasons (42, 43). The increased levels of kinetochore BubR1 may actually limit chromosome aberrations in Aurora B-overexpressing cells due to the function of this SAC component in protecting against aneuploidy (44). However, we were initially surprised by the fact that spleen tumors were much more frequent than epithelial tumors, such as lung or liver cancers commonly found in other CIN models (4, 42, 45). These results may be a consequence of the possible role of Aurora B in modulating p53 activity *in vivo*. Aurora A and Aurora B are known to phosphorylate and inactivate p53 in cultured cells, resulting in decreased expression of its transcriptional targets (24, 25, 46). Indeed, Aurora B deficiency leads to enhanced expression of $p21^{Cip1}$, resulting in aberrant Cdk activity and cell cycle progression (26, 47). These results are also in agreement with an inverse correlation between Aurora B and $p21^{Cip1}$ mRNA levels in human B-ALL (Fig. 8).

Our data suggest that Aurora B is indeed a critical regulator of p53 *in vivo* and that overexpression of this kinase in cancer may lead to impaired p53 function and reduced levels of p53 targets such as the cell cycle inhibitor $p21^{Cip1}$. Although our data do not demonstrate a causal role for aneuploidy or defective p53 target expression in tumor formation in Aurora B-overexpressing mice, it is likely that these two factors may contribute to tumor formation in specific cell types. Since Aurora kinases are currently considered important cancer targets (48, 49), our data also suggest a possible effect of Aurora inhibitors in restoring p53 activity at least in some specific tumors.

ACKNOWLEDGMENTS

We are indebted to members of the Animal Facility, as well as the Histopathology, Molecular Imaging, and Confocal Microscopy facilities of the Spanish National Cancer Research Center (CNIO) for their excellent technical support.

A.G.-L. and M.T. were supported by fellowships from the Spanish Ministry of Economy and Competitiveness (MINECO) and Fundación La Caixa, respectively. This work was supported by grants from the MINECO (PI14/0027 to I.P.D.C. and SAF2012-38215 to M.M.), Fundación Ramón Areces, the OncoCycle Program (S2010/BMD-2470) from the Comunidad de Madrid, the OncoBIO Consolider-Ingenio Program (SAF2014-57791-REDC) and Red Temática CellSYS (BFU2014-52125-REDT) from the MINECO, and grants from Worldwide Cancer Research (WCR 15-0278) and the European Union Seventh Framework Programme (MitoSys project; HEALTH-F5-2010-241548). Work in the W.C.E. laboratory was supported by The Wellcome Trust, of which W.C.E. is a Principal Research Fellow (grant number 073915).

REFERENCES

1. **Albertson DG, Collins C, McCormick F, Gray JW.** 2003. Chromosome aberrations in solid tumors. Nat Genet **34:**369–376. http://dx.doi.org/10.1038/ng1215.
2. **Pérez de Castro I, de Cárcer G, Malumbres M.** 2007. A census of mitotic cancer genes: new insights into tumor cell biology and cancer therapy. Carcinogenesis **28:**899–912.
3. **Holland AJ, Cleveland DW.** 2009. Boveri revisited: chromosomal instability, aneuploidy and tumorigenesis. Nat Rev Mol Cell Biol **10:**478–487. http://dx.doi.org/10.1038/nrm2718.
4. **Schvartzman JM, Sotillo R, Benezra R.** 2010. Mitotic chromosomal instability and cancer: mouse modelling of the human disease. Nat Rev Cancer **10:**102–115. http://dx.doi.org/10.1038/nrc2781.
5. **Carmena M, Ruchaud S, Earnshaw WC.** 2009. Making the Auroras glow: regulation of Aurora A and B kinase function by interacting proteins. Curr Opin Cell Biol **21:**796–805. http://dx.doi.org/10.1016/j.ceb.2009.09.008.
6. **Chan CS, Botstein D.** 1993. Isolation and characterization of chromosome-gain and increase-in-ploidy mutants in yeast. Genetics **135:**677–691.
7. **Carmena M, Wheelock M, Funabiki H, Earnshaw WC.** 2012. The chromosomal passenger complex (CPC): from easy rider to the godfather of mitosis. Nat Rev Mol Cell Biol **13:**789–803. http://dx.doi.org/10.1038/nrm3474.
8. **Lampson MA, Cheeseman IM.** 2011. Sensing centromere tension: Aurora B and the regulation of kinetochore function. Trends Cell Biol **21:**133–140. http://dx.doi.org/10.1016/j.tcb.2010.10.007.
9. **Gregan J, Polakova S, Zhang L, Tolić-Nørrelykke IM, Cimini D.** 2011. Merotelic kinetochore attachment: causes and effects. Trends Cell Biol **21:**374–381. http://dx.doi.org/10.1016/j.tcb.2011.01.003.
10. **Gay G, Courtheoux T, Reyes C, Tournier S, Gachet Y.** 2012. A stochastic model of kinetochore-microtubule attachment accurately describes fission yeast chromosome segregation. J Cell Biol **196:**757–774. http://dx.doi.org/10.1083/jcb.201107124.
11. **Munoz-Barrera M, Monje-Casas F.** 2014. Increased Aurora B activity causes continuous disruption of kinetochore-microtubule attachments and spindle instability. Proc Natl Acad Sci U S A **111:**E3996–E4005. http://dx.doi.org/10.1073/pnas.1408017111.
12. **Ota T, Suto S, Katayama H, Han ZB, Suzuki F, Maeda M, Tanino M, Terada Y, Tatsuka M.** 2002. Increased mitotic phosphorylation of histone H3 attributable to AIM-1/Aurora-B overexpression contributes to chromosome number instability. Cancer Res **62:**5168–5177.
13. **Zhang D, Hirota T, Marumoto T, Shimizu M, Kunitoku N, Sasayama T, Arima Y, Feng L, Suzuki M, Takeya M, Saya H.** 2004. Cre-loxP-controlled periodic Aurora-A overexpression induces mitotic abnormalities and hyperplasia in mammary glands of mouse models. Oncogene **23:**8720–8730. http://dx.doi.org/10.1038/sj.onc.1208153.
14. **Bischoff JR, Anderson L, Zhu Y, Mossie K, Ng L, Souza B, Schryver B, Flanagan P, Clairvoyant F, Ginther C, Chan CS, Novotny M, Slamon DJ, Plowman GD.** 1998. A homologue of *Drosophila* aurora kinase is oncogenic and amplified in human colorectal cancers. EMBO J **17:**3052–3065. http://dx.doi.org/10.1093/emboj/17.11.3052.
15. **Araki K, Nozaki K, Ueba T, Tatsuka M, Hashimoto N.** 2004. High expression of Aurora-B/Aurora and Ipll-like midbody-associated protein (AIM-1) in astrocytomas. J Neurooncol **67:**53–64. http://dx.doi.org/10.1023/B:NEON.0000021784.33421.05.
16. **Chieffi P, Troncone G, Caleo A, Libertini S, Linardopoulos S, Tramontano D, Portella G.** 2004. Aurora B expression in normal testis and seminomas. J Endocrinol **181:**263–270. http://dx.doi.org/10.1677/joe.0.1810263.
17. **Smith SL, Bowers NL, Betticher DC, Gautschi O, Ratschiller D, Hoban PR, Booton R, Santibáñez-Koref MF, Heighway J.** 2005. Overexpression of aurora B kinase (AURKB) in primary non-small cell lung carcinoma is frequent, generally driven from one allele, and correlates with the level of genetic instability. Br J Cancer **93:**719–729. http://dx.doi.org/10.1038/sj.bjc.6602779.
18. **Sorrentino R, Libertini S, Pallante PL, Troncone G, Palombini L, Bavetsias V, Spalletti-Cernia D, Laccetti P, Linardopoulos S, Chieffi P, Fusco A, Portella G.** 2005. Aurora B overexpression associates with the thyroid carcinoma undifferentiated phenotype and is required for thyroid carcinoma cell proliferation. J Clin Endocrinol Metab **90:**928–935. http://dx.doi.org/10.1210/jc.2004-1518.
19. **Vischioni B, Oudejans JJ, Vos W, Rodriguez JA, Giaccone G.** 2006. Frequent overexpression of aurora B kinase, a novel drug target, in non-small cell lung carcinoma patients. Mol Cancer Ther **5:**2905–2913. http://dx.doi.org/10.1158/1535-7163.MCT-06-0301.
20. **Gibson SE, Zeng WF, Weil RJ, Prayson RA.** 2008. Aurora B kinase expression in ependymal neoplasms. Appl Immunohistochem Mol Morphol **16:**274–278. http://dx.doi.org/10.1097/PAI.0b013e318126bff5.
21. **Hegyi K, Egervári K, Sándor Z, Méhes G.** 2012. Aurora kinase B expres-

sion in breast carcinoma: cell kinetic and genetic aspects. Pathobiology **79:**314–322. http://dx.doi.org/10.1159/000338082.
22. **Tanaka S, Arii S, Yasen M, Mogushi K, Su NT, Zhao C, Imoto I, Eishi Y, Inazawa J, Miki Y, Tanaka H.** 2008. Aurora kinase B is a predictive factor for the aggressive recurrence of hepatocellular carcinoma after curative hepatectomy. Br J Surg **95:**611–619. http://dx.doi.org/10.1002/bjs.6011.
23. **Carter SL, Eklund AC, Kohane IS, Harris LN, Szallasi Z.** 2006. A signature of chromosomal instability inferred from gene expression profiles predicts clinical outcome in multiple human cancers. Nat Genet **38:**1043–1048. http://dx.doi.org/10.1038/ng1861.
24. **Wu L, Ma CA, Zhao Y, Jain A.** 2011. Aurora B interacts with NIR-p53, leading to p53 phosphorylation in its DNA-binding domain and subsequent functional suppression. J Biol Chem **286:**2236–2244. http://dx.doi.org/10.1074/jbc.M110.174755.
25. **Gully CP, Velazquez-Torres G, Shin JH, Fuentes-Mattei E, Wang E, Carlock C, Chen J, Rothenberg D, Adams HP, Choi HH, Guma S, Phan L, Chou PC, Su CH, Zhang F, Chen JS, Yang TY, Yeung SC, Lee MH.** 2012. Aurora B kinase phosphorylates and instigates degradation of p53. Proc Natl Acad Sci U S A **109:**E1513–E1522. http://dx.doi.org/10.1073/pnas.1110287109.
26. **Trakala M, Fernandez-Miranda G, Perez de Castro I, Heeschen C, Malumbres M.** 2013. Aurora B prevents delayed DNA replication and premature mitotic exit by repressing $p21^{Cip1}$. Cell cycle **12:**1030–1041. http://dx.doi.org/10.4161/cc.24004.
27. **Samejima K, Ogawa H, Cooke CA, Hudson DF, Hudson D, Macisaac F, Ribeiro SA, Vagnarelli P, Cardinale S, Kerr A, Lai F, Ruchaud S, Yue Z, Earnshaw WC.** 2008. A promoter-hijack strategy for conditional shutdown of multiply spliced essential cell cycle genes. Proc Natl Acad Sci U S A **105:**2457–2462. http://dx.doi.org/10.1073/pnas.0712083105.
28. **Beard C, Hochedlinger K, Plath K, Wutz A, Jaenisch R.** 2006. Efficient method to generate single-copy transgenic mice by site-specific integration in embryonic stem cells. Genesis **44:**23–28. http://dx.doi.org/10.1002/gene.20180.
29. **García-Higuera I, Manchado E, Dubus P, Cañamero M, Méndez J, Moreno S, Malumbres M.** 2008. Genomic stability and tumour suppression by the APC/C cofactor Cdh1. Nat Cell Biol **10:**802–811. http://dx.doi.org/10.1038/ncb1742.
30. **Perera D, Tilston V, Hopwood JA, Barchi M, Boot-Handford RP, Taylor SS.** 2007. Bub1 maintains centromeric cohesion by activation of the spindle checkpoint. Dev Cell **13:**566–579. http://dx.doi.org/10.1016/j.devcel.2007.08.008.
31. **Kang H, Chen IM, Wilson CS, Bedrick EJ, Harvey RC, Atlas SR, Devidas M, Mullighan CG, Wang X, Murphy M, Ar K, Wharton W, Borowitz MJ, Bowman WP, Bhojwani D, Carroll WL, Camitta BM, Reaman GH, Smith MA, Downing JR, Hunger SP, Willman CL.** 2010. Gene expression classifiers for relapse-free survival and minimal residual disease improve risk classification and outcome prediction in pediatric B-precursor acute lymphoblastic leukemia. Blood **115:**1394–1405. http://dx.doi.org/10.1182/blood-2009-05-218560.
32. **Harvey RC, Mullighan CG, Wang X, Dobbin KK, Davidson GS, Bedrick EJ, Chen IM, Atlas SR, Kang H, Ar K, Wilson CS, Wharton W, Murphy M, Devidas M, Carroll AJ, Borowitz MJ, Bowman WP, Downing JR, Relling M, Yang J, Bhojwani D, Carroll WL, Camitta B, Reaman GH, Smith M, Hunger SP, Willman CL.** 2010. Identification of novel cluster groups in pediatric high-risk B-precursor acute lymphoblastic leukemia with gene expression profiling: correlation with genome-wide DNA copy number alterations, clinical characteristics, and outcome. Blood **116:**4874–4884. http://dx.doi.org/10.1182/blood-2009-08-239681.
33. **Schwenk F, Baron U, Rajewsky K.** 1995. A cre-transgenic mouse strain for the ubiquitous deletion of loxP-flanked gene segments including deletion in germ cells. Nucleic Acids Res **23:**5080–5081. http://dx.doi.org/10.1093/nar/23.24.5080.
34. **Fernandez-Miranda G, Trakala M, Martin J, Escobar B, Gonzalez A, Ghyselinck NB, Ortega S, Canamero M, Perez de Castro I, Malumbres M.** 2011. Genetic disruption of aurora B uncovers an essential role for aurora C during early mammalian development. Development **138:**2661–2672. http://dx.doi.org/10.1242/dev.066381.
35. **Carmena M, Earnshaw WC.** 2003. The cellular geography of aurora kinases. Nat Rev Mol Cell Biol **4:**842–854. http://dx.doi.org/10.1038/nrm1245.
36. **Adams RR, Maiato H, Earnshaw WC, Carmena M.** 2001. Essential roles of Drosophila inner centromere protein (INCENP) and aurora B in histone H3 phosphorylation, metaphase chromosome alignment, kinetochore disjunction, and chromosome segregation. J Cell Biol **153:**865–880. http://dx.doi.org/10.1083/jcb.153.4.865.
37. **Ditchfield C, Johnson VL, Tighe A, Ellston R, Haworth C, Johnson T, Mortlock A, Keen N, Taylor SS.** 2003. Aurora B couples chromosome alignment with anaphase by targeting BubR1, Mad2, and Cenp-E to kinetochores. J Cell Biol **161:**267–280. http://dx.doi.org/10.1083/jcb.200208091.
38. **Hauf S, Cole RW, LaTerra S, Zimmer C, Schnapp G, Walter R, Heckel A, van Meel J, Rieder CL, Peters JM.** 2003. The small molecule Hesperadin reveals a role for Aurora B in correcting kinetochore-microtubule attachment and in maintaining the spindle assembly checkpoint. J Cell Biol **161:**281–294. http://dx.doi.org/10.1083/jcb.200208092.
39. **Nguyen HG, Makitalo M, Yang D, Chinnappan D, St Hilaire C, Ravid K.** 2009. Deregulated Aurora-B induced tetraploidy promotes tumorigenesis. FASEB J **23:**2741–2748. http://dx.doi.org/10.1096/fj.09-130963.
40. **Tatsuka M, Katayama H, Ota T, Tanaka T, Odashima S, Suzuki F, Terada Y.** 1998. Multinuclearity and increased ploidy caused by overexpression of the aurora- and Ipl1-like midbody-associated protein mitotic kinase in human cancer cells. Cancer Res **58:**4811–4816.
41. **Fant X, Samejima K, Carvalho A, Ogawa H, Xu Z, Yue Z, Earnshaw WC, Ruchaud S.** 2010. Use of DT40 conditional-knockout cell lines to study chromosomal passenger protein function. Biochem Soc Trans **38:**1655–1659. http://dx.doi.org/10.1042/BST0381655.
42. **Ricke RM, Jeganathan KB, van Deursen JM.** 2011. Bub1 overexpression induces aneuploidy and tumor formation through Aurora B kinase hyperactivation. J Cell Biol **193:**1049–1064. http://dx.doi.org/10.1083/jcb.201012035.
43. **Ricke RM, van Deursen JM.** 2013. Aneuploidy in health, disease, and aging. J Cell Biol **201:**11–21. http://dx.doi.org/10.1083/jcb.201301061.
44. **Baker DJ, Dawlaty MM, Wijshake T, Jeganathan KB, Malureanu L, van Ree JH, Crespo-Diaz R, Reyes S, Seaburg L, Shapiro V, Behfar A, Terzic A, van de Sluis B, van Deursen JM.** 2013. Increased expression of BubR1 protects against aneuploidy and cancer and extends healthy lifespan. Nat Cell Biol **15:**96–102. http://dx.doi.org/10.1038/ncb2643.
45. **Sotillo R, Hernando E, Díaz-Rodríguez E, Teruya-Feldstein J, Cordón-Cardo C, Lowe SW, Benezra R.** 2007. Mad2 overexpression promotes aneuploidy and tumorigenesis in mice. Cancer Cell **11:**9–23. http://dx.doi.org/10.1016/j.ccr.2006.10.019.
46. **Katayama H, Sasai K, Kawai H, Yuan ZM, Bondaruk J, Suzuki F, Fujii S, Arlinghaus RB, Czerniak BA, Sen S.** 2004. Phosphorylation by aurora kinase A induces Mdm2-mediated destabilization and inhibition of p53. Nat Genet **36:**55–62. http://dx.doi.org/10.1038/ng1279.
47. **Kumari G, Ulrich T, Krause M, Finkernagel F, Gaubatz S.** 2014. Induction of $p21^{Cip1}$ protein and cell cycle arrest after inhibition of Aurora B kinase is attributed to aneuploidy and reactive oxygen species. J Biol Chem **289:**16072–16084. http://dx.doi.org/10.1074/jbc.M114.555060.
48. **Domenech E, Malumbres M.** 2013. Mitosis-targeting therapies: a troubleshooting guide. Curr Opin Pharmacol **13:**519–528. http://dx.doi.org/10.1016/j.coph.2013.03.011.
49. **Lens SM, Voest EE, Medema RH.** 2010. Shared and separate functions of polo-like kinases and aurora kinases in cancer. Nat Rev Cancer **10:**825–841. http://dx.doi.org/10.1038/nrc2964.